Journal of Dental Research
2015, Vol. 94(12) 1740–1747

DOI: 10.1177/0022034515606900
jdr.sagepub.com

Ameloblast Modulation and Transport of Cl^-, Na^+, and K^+ during Amelogenesis

A.L.J.J. Bronckers[1], D. Lyaruu[1], R. Jalali[1], J.F. Medina[2], B. Zandieh-Doulabi[1], and P.K. DenBesten[3]

Abstract

Ameloblasts express transmembrane proteins for transport of mineral ions and regulation of pH in the enamel space. Two major transporters recently identified in ameloblasts are the Na^+K^+-dependent calcium transporter NCKX4 and the Na^+-dependent HPO_4^{2-} (Pi) cotransporter NaPi-2b. To regulate pH, ameloblasts express anion exchanger 2 (Ae2a,b), chloride channel Cftr, and amelogenins that can bind protons. Exposure to fluoride or null mutation of *Cftr, Ae2a,b*, or *Amelx* each results in formation of hypomineralized enamel. We hypothesized that enamel hypomineralization associated with disturbed pH regulation results from reduced ion transport by NCKX4 and NaPi-2b. This was tested by correlation analyses among the levels of Ca, Pi, Cl, Na, and K in forming enamel of mice with null mutation of *Cftr, Ae2a,b*, and *Amelx*, according to quantitative x-ray electron probe microanalysis. Immunohistochemistry, polymerase chain reaction analysis, and Western blotting confirmed the presence of apical NaPi-2b and Nckx4 in maturation-stage ameloblasts. In wild-type mice, K levels in enamel were negatively correlated with Ca and Cl but less negatively or even positively in fluorotic enamel. Na did not correlate with P or Ca in enamel of wild-type mice but showed strong positive correlation in fluorotic and nonfluorotic *Ae2a,b*- and *Cftr*-null enamel. In hypomineralizing enamel of all models tested, 1) Cl^- was strongly reduced; 2) K^+ and Na^+ accumulated (Na^+ not in *Amelx*-null enamel); and 3) modulation was delayed or blocked. These results suggest that a Na^+K^+-dependent calcium transporter (likely NCKX4) and a Na^+-dependent Pi transporter (potentially NaPi-2b) located in ruffle-ended ameloblasts operate in a coordinated way with the pH-regulating machinery to transport Ca^{2+}, Pi, and bicarbonate into maturation-stage enamel. Acidification and/or associated physicochemical/electrochemical changes in ion levels in enamel fluid near the apical ameloblast membrane may reduce the transport activity of mineral transporters, which results in hypomineralization.

Keywords: SLC24A4, SLC34A2, chloride-bicarbonate exchangers, dental enamel hypomaturation, fluorosis, electron probe microanalysis

Introduction

Hypomineralization of enamel is a developmental defect in which the enamel is deposited in its usual thickness but fails to fully mineralize. External or genetic factors—including fluoride, disruption of pH regulators, mutations in MMP20, KLK4, and mineral ion transporters—can give rise to formation of hypomineralized enamel (DenBesten and Li 2011; Wright et al. 2015).

The molecular mechanism that leads to enamel hypomineralization is not clear. In fluorotic enamel, the presence of multiple hypermineralized lines could form a physical barrier for ions to diffuse into deeper layers (Lyaruu et al. 2014). Such hypermineralized lines, however, are not formed in nonfluorotic *Cftr*- and *Ae2a,b*-null mice, which suggests that also other mechanisms are responsible for developing hypomineralization.

During the secretory stage of amelogenesis, thin hydroxyapatite crystals are formed within a protein-rich matrix (Smith 1998). During maturation stage, the matrix is removed, and crystals expand in thickness. A unique phenomenon during the maturation stage is that ameloblasts modulate (Josephsen et al. 2010; Takano and Ozawa 1980), involving repetitive pH changes in the forming enamel seen as acid (pH 6.0) and neutral (pH 7.2) bands. When modulation is delayed or disrupted, enamel mineralization is reduced (DenBesten et al. 1985; Smith et al. 1993). The biological significance of modulation and the molecular mechanism controlling ameloblast modulation are unknown. To mineralize enamel, ameloblasts must transport Ca^{2+} and HPO_4^{2-} (Pi) into the enamel space using transmembrane transporter molecules, including members of sodium-calcium exchanger family (solute carrier 8A/SLC8A; Okumura et al. 2010; Lacruz et al. 2011; Lacruz et al. 2012; Lacruz et al. 2013) and sodium-potassium-calcium exchangers (NCKX/SLC24A family; Hu et al. 2012; Wang et al. 2014). The NCKX family has the highest calcium transport capacity, and it functions bidirectionally, depending on the electrochemical

[1]Department of Oral Cell Biology, Academic Centre for Dentistry Amsterdam, University of Amsterdam, and MOVE Research Institute, VU University Amsterdam, Amsterdam, Netherlands
[2]Division of Gene Therapy and Hepatology, School of Medicine/CIMA, University of Navarra, and CIBERehd, Pamplona, Spain
[3]Department of Oral Sciences, University of California, San Francisco, CA, USA

A supplemental appendix to this article is published electronically only at http://jdr.sagepub.com/supplemental.

Corresponding Author:
A.L.J.J. Bronckers, Department of Oral Cell Biology, ACTA, Gustav Mahlerlaan 3004, 1081 LA Amsterdam, The Netherlands.
Email: a.bronckers@acta.nl

gradient over the plasma membrane (Stephan et al. 2011). Mouse ameloblasts express transcripts of all 6 *Nckx* isoforms, of which *Nckx4* (*Slc24a4*) is by far the most highly expressed one during late maturation stage (Hu et al. 2012). Mutation of *NCKX* in humans or its deletion in mice results in formation of poorly calcified enamel (Parry et al. 2013; Wang et al. 2014). Sodium phosphate cotransporters (NaPi/SLC34A family) are electrogenic transmembrane proteins that cotransport divalent phosphate with sodium from the extracellular fluid into the cell (Schiavi et al. 2012; Forster et al. 2013). NaPi-2b (SLC34A2) is a sodium-dependent transporter that cotransports Na^+ with Pi in many tissues, such as salivary glands, liver, and intestine (Forster et al. 2013). Maturation ameloblasts highly express transcripts for NaPi-2b (Lacruz et al. 2012). A null mutation of *NaPi-2b* is embryonic lethal (Shibasaki et al. 2009). In various types of transport epithelia (e.g., renal and intestinal epithelia), the activity of Ca^{2+}, Pi transporters, and bicarbonate secretors in the apical plasma membranes depends on K^+ and/or Na^+ levels of the luminal fluid; these levels continuously change when the glandular fluid moves through the ducts and is eventually secreted into an orifice. In forming enamel, however, the luminal space forms a closed compartment in which mineral ions are withdrawn from luminal fluid to form crystals. Enamel also contains Cl^-, K^+, and Na^+ retained in association with apatite minerals (Söremark and Grön 1966; Shaw and Yen 1972; Aoba et al. 1992; Lundgren et al. 1998). In *Cftr*-null mice, Na and K levels in enamel are increased (Gawenis et al. 2001; Arquitt et al. 2002). We reasoned that levels of K^+ and Na^+ in forming enamel reflect the transport activity of $NCKX_4$ and NaPi-2b.

By quantitative x-ray electron microscopy, we measured trace elements and minerals in forming enamel in mouse models in which enamel is hypomineralized by defects in pH regulation, including mice exposed to fluoride or with null mutation of *Cftr, Ae2a,b*, and *Amelx* (Lyaruu et al. 2008; Lyaruu et al. 2014; Bronckers et al. 2015; Guo et al. 2015). We tested the hypothesis that ameloblasts use trace elements to mineralize enamel and that changes in levels of trace elements reflect changes in transport activity leading to enamel hypomineralization.

Materials and Methods

Animals, Tissues, and Tissue Processing

The mouse strains and procedures for these studies have been described (Lyaruu et al. 2014; Bronckers et al. 2015; Guo et al. 2015). In short, for each genotypic mouse strain, 2 groups of wild-type mice and 2 groups of null mutants were analyzed: 1 of each 2 groups was exposed to drinking water with 100 mg/L of fluoride for 6 wk; the other was not exposed. Each group consisted of a minimum of 3 mice. Some mice were injected with calcein 30 min prior to sacrifice (Bronckers et al. 2015) to reveal modulation bands. All procedures were approved by the national committees for animal health care of the involved departments.

Electron Probe Microanalysis

Quantitative elemental analysis of lower incisor enamel was carried out by electron probe microanalysis as previously described (Lyaruu et al. 2014; Appendix Fig. 1). Measurements were made at the secretory, mid-, and late-maturation stages, halfway through the enamel layer.

Western Blotting and Immunohistochemistry

Two rabbit anti-NCKX4 antibodies were purchased: the first from Protein Tech Group Inc. (Chicago, IL, USA; 18992-1-AP; Hu et al. 2012) raised against a (not specified) peptide sequence at the N-terminal end, the other from Abcam (Cambridge, UK; ab136968; Wang et al. 2014; Wang et al. 2015) raised against a (not specified) internal region. Also for NaPi-2b, 2 rabbit antibodies were used: the first against the C-terminal end (CQVEV LSMKALSNTTVF, amino acids 681 to 697; donated by Dr. Y. Sabbagh, Sanofi, Framingham, MA, USA), the second (donated by Dr. I. Forster, University of Zürich, Switzerland) raised to the N-terminal end (MAPWPELEN AQPNPGKC, amino acids 1 to 17; Hilfiker et al. 1998). The first antibody to NaPi-2b reacted with adult small intestine epithelium of wild-type mice but not that of *NaPi-2b*-null mice, validating its specificity (Schiavi et al. 2012). Real-time polymerase chain reaction and Western blotting were carried out as reported (Jalali et al. 2014; Jalali et al. 2015; Appendix Figs. 2, 3). Dewaxed paraffin sections were incubated with the rabbit primary antibodies (1:200 dilution), subsequently incubated with goat anti-rabbit peroxidase-conjugated IgG (Envision; Dakopatt, Glostrup, Denmark) or goat anti-rabbit Alexa Fluor 488–conjugated IgG (2 ug/mL; Molecular Probes, Eugene, OR, USA). Sections were counterstained with hematoxylin or propidium iodine (5 ug/mL). Antibody to N-terminal NCKX4 and C-terminal NaPi-2b required antigen retrieval in hot 10mM Tris–0.5mM ethylenediaminetetraacetic acid (EDTA) (pH 9) solution before immunostaining. For negative controls, the primary antibodies were replaced by matched rabbit nonimmune IgG.

Calculations and Statistics

Element levels were calculated as mol/kg or mmol/kg and presented as means and standard deviation. Statistical differences between groups at the same developmental stage were analyzed by analysis of variance according to Microsoft Excel 10 (Redmond, WA, USA), with significance established at $P < 0.05$. Correlations were analyzed by linear regression via Graphpad Instat 3 software. The correlation factor (r) varies between 0 (no correlation) and 1 (complete correlation). Values for $r \leq 0.35$ are defined as low/weak, $0.35 < r \leq 0.67$ as moderate, $0.68 < r \leq 0.89$ as strong, and $0.90 \leq r \leq 1.00$ as very strong. The P value presented by the slope values indicates whether the slope angle is significantly different from 0 ($P < 0.05$).

Results

Maturation Ameloblasts Express Nckx4 and NaPi-2b

A pilot study identified transcripts for *Nckx4* and *NaPi-2b* in enamel organs of wild-type mice (Appendix Fig. 2). Western

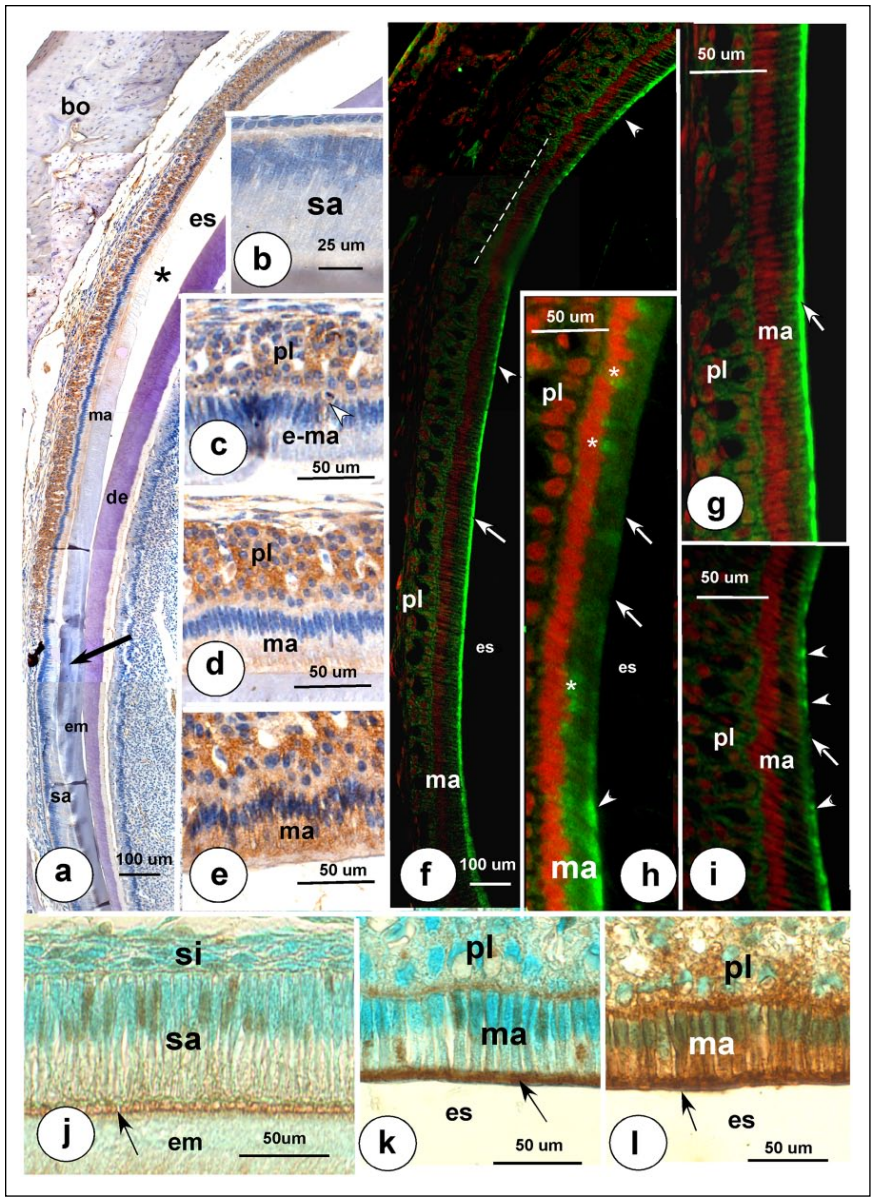

Figure 1. Immunolocalization of Nckx4 (**a–i**) and NaPi-2b (**j–l**) in enamel organs of upper incisors. (a, f–i) Incisal end at the top, cervical loop end at the bottom. (a–e) Immunostaining with anti-Nckx4 raised to N-terminal sequence (peroxidase, brown reaction product). Secretory-stage ameloblasts (sa) and stratum intermedium (si) are negative for Nckx4 (b). Arrow (a) indicates approximate end of secretion stage. The first (intracellular) staining for Nckx4 is apparent in papillary layer (a, c), while early maturation–stage ameloblasts (e-ma) are immunonegative. Arrowhead (c) points at dark granules characteristic for transitional stage. As enamel matrix becomes EDTA soluble (asterisks; a), maturation ameloblasts (ma) become positive (d), and staining intensity increases progressively (e). (f–i) Immunofluoresent staining of maturation zone with antibodies to internal part of Nckx4. (f) A strong positive staining (Nckx4: green; nuclei: red) is located in the apical membranes (white arrow). The broken white line near the top indicates the gap area with weak or negative staining (f). Arrowhead below gap indicates a gradual weaker and irregular apical staining for Nckx4 shortly before the gap, while younger cells (more down) show strong apical staining. (h) The last positive cell (arrowhead) at the start of a negative gap (arrows). Cells marked with asterisk show weak supranuclear staining. In cells more incisally from the gap (i), apical staining reappears (f, i). Staining with anti-NaPi-2b shows with both antibodies a weak apical staining of the secretory ameloblasts (sa) as well as in some nuclei (j). Early (k) and late (l) maturation–stage ameloblasts stain intensely for NaPi-2b, intracellularly and very prominent over the apical plasma membranes. Also, papillary cells stain for NaPi-2b. em, enamel matrix; es, enamel space. Only shown, anti-NaPi-2b raised against C-terminal end. This figure is available in color online at http://jdr.sagepub.com.

blots stained with anti-NaPi-2b and anti-Nckx4 showed immunopositive bands in enamel organ extracts of the expected sizes (Appendix Fig. 3). Both antibodies to NCKX4 stained postsecretory ameloblasts with basically the same distribution. The antibody against the N-terminal end reacted predominantly intracellularly (Fig. 1a–e); the one against the internal sequence stained ameloblasts apically (Fig. 1f–i). Secretory ameloblasts were negative (Fig. 1b). The first intracellular staining was detected in the papillary layer at early maturation (Fig. 1a–c) slightly later in maturation ameloblasts. This staining increased in intensity when matrix was almost gone (Fig. 1d, e). In ameloblasts, the apical staining formed a strong continuous line (Fig. 1f, g) that occasionally became interrupted in a small group of ameloblasts with weak or no staining (Fig. 1f, h, i). For NaPi-2b, both antibodies stained the apical membranes in ameloblasts (Fig. 1j–l) and, more weakly, the papillary layer (Fig. 1i). Staining was weak to moderate in secretory stage but strong in maturation stage (Fig. 1j–l). When the first antibody was replaced by nonimmune IgG, cells did not stain (not shown).

Potassium Correlates Negatively with Calcium during Normal Mineralization but Loses Correlation or Correlates Positively during Enamel Hypomineralization

Figure 2a presents the levels of K, Na, P, and S measured in wild-type enamel plotted as function of calcium levels. Unlike what was expected based on the 1:1:4 stoichiometric transport of Ca^{2+}, K^{+}, and Na^{+} by Nckx4, K levels in maturation-stage wild-type enamel were at least 100-fold lower than Ca and decreased during maturation, indicated by the strong negative correlation between K and Ca ($r = –0.84$; Fig. 2a). Very strong positive correlations were found between Ca and P ($r = 0.99$) and between Ca and Cl ($r = 0.98$). Very strong negative correlations were found between Ca and S (considered a measure for enamel matrix; $r = –0.93$). We next analyzed these correlations in enamel of experimental mice that develop hypomineralizing enamel. The correlations between K and Ca

(Fig. 2b, shown for *Ae2a,b*-null mice) and between K and Cl (Fig. 2c) changed in a similar pattern. Correlations that were negative in wild-type enamel became less negative in fluorotic wild type (i.e., curve slopes became less steep in fluorotic or mutant enamel). In most null mutants, these correlations were very weak or turned sometimes positive (e.g., Fig. 2c).

Figure 3 presents levels of Ca, Cl, K, and Na in late-maturation stage enamel. All treatments reduced calcium (Fig. 3a). Most strikingly was a reduction in the level of Cl (Fig. 3b), which reached lowest levels in fluorotic null enamel. K levels in all mutant and fluorotic enamel at late maturation were 2- to 5-fold higher than in wild-type controls (Fig. 3c). Na levels increased in all experimental groups (except in *Amelx*-null mice), particularly in fluorotic teeth of null mutant mice (Fig. 3d).

When Buffering Is Reduced, Potassium Accumulates and Enamel Hypomineralizes

During maturation stage, protons released by mineral accretion (Ca) are likely buffered by bicarbonates in exchange for (luminal) Cl^-. In enamel of wild-type mice, Cl levels per unit of Ca were high but progressively decreased in experimental mice as enamel hypomineralized (Fig. 4a), most substantially in fluorotic null mice. K levels per unit of Ca, however, increased 2- to 4.5-fold in hypomineralizing enamel in comparison with wild-type enamel, and K per unit of Cl increased 6- to 22-fold (Fig. 4b, c). These results indicate that poor buffering by ameloblasts decreased the mineral accretion during maturation and increased accumulation of K^+.

Sodium Levels Are Positively Correlated with Phosphate (and Calcium) in Hypomineralizing Enamel When Sodium Resorption Is Inhibited

To examine involvement of NaPi-2b in transport of Pi, correlation analysis was done between Na and P. In nonfluorotic and fluorotic wild-type enamel, no correlation was found between Na and P (slope: 0.7 and –18 mmol Na/mol P, respectively; Fig. 4d). However, Na was positively correlated with P (and Ca) in nonfluorotic ($r = 0.80$; slope: 38 mmol Na/mol P; $P = 0.01$) and fluorotic *Ae2a,b*-null enamel ($r = 0.91$, slope: 111 mmol Na/mol P; $P = 0.01$). Similar correlations between Na and P were obtained in nonfluorotic and fluorotic *Cftr*-null enamel (not shown).

Changes in Ameloblast Modulation at Low Cl^- and High K^+ Levels

After injection of calcein into wild-type mice, 3 sets of fluorescent (double) bands were detected at the surface of forming enamel. The first set of fluorescent bands at the beginning of maturation was intense and broad, but the second and third sets were much weaker and narrower (Fig. 4e 1, 2). In enamel of *Amelx*$^{-/-}$ mice, all 3 fluorescent bands were narrow and of equal low intensity (Fig. 4e 3). No fluorescent bands were seen in *Ae2a,b*-null enamel after calcein injection (Fig. 4e 4), similar to what was previously reported for *Cftr*$^{-/-}$ enamel (Bronckers et al. 2015). A summary of ameloblast modulation and changes in enamel composition is presented in Appendix Table 2. It shows that the lower Cl^- and higher K^+, the more modulation is affected.

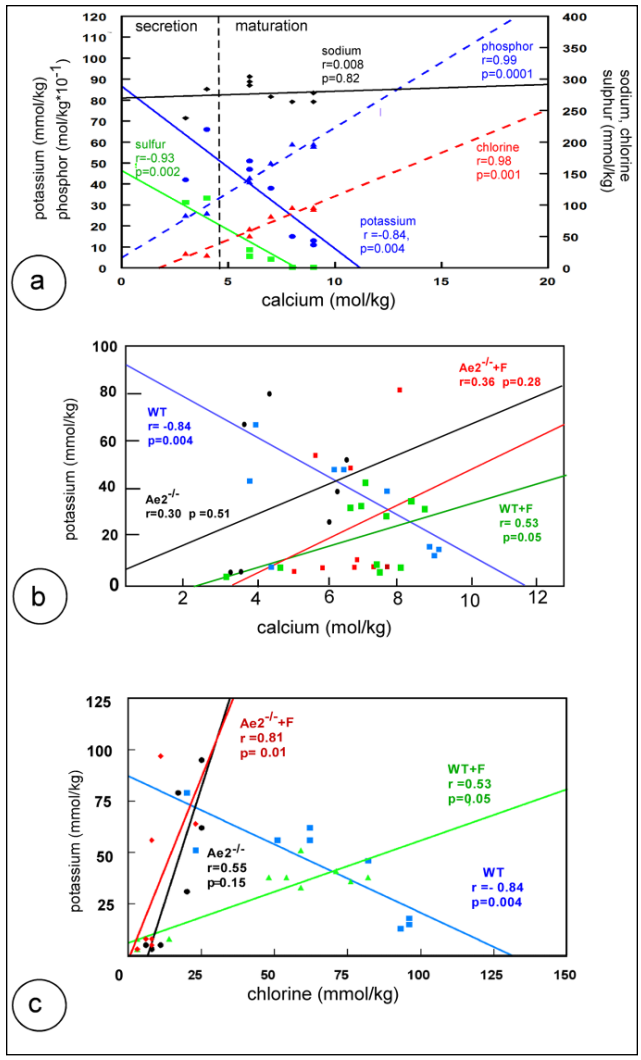

Figure 2. Changes in composition of developing fluorotic and nonfluorotic enamel of lower incisors in wild-type and *Ae2*-null mutant mice. (**a**) Correlation analysis between various trace elements as function of mineralization (Ca) or buffer capacity (Cl increase) in wild-type enamel. Sodium (Na), potassium (K), phosphorus (P), sulfur (S), and chlorine (Cl) were plotted against calcium (Ca). K vs Ca (blue solid line); $r = –0.84$; slope, –8.0 mmol K/mol Ca; $P = 0.004$. Na vs Ca (black solid line); $r = 0.008$; slope, 0.9 mmol Na/mol Ca; $P = 0.82$. Cl vs Ca (red broken line); $r = 0.98$; slope, 15 mmol Cl/mol Ca; $P = 0.001$. S vs Ca (green solid line); $r = –0.93$; slope, –21 mmol S/mol Ca; $P = 0.002$. P vs Ca (blue broken line); $r = 0.99$; slope, 0.7 mol P/mol Ca; $P = 0.0001$. (**b**) Correlations between calcium and potassium in Ae2 group. Wild-type enamel (WT; blue line), fluorotic wild-type (WT+F; green line), *Ae2a,b*-null enamel (*Ae2*-null; black line), and fluorotic *Ae2*-null enamel (*Ae2*-null+F; red line). WT: $r = –0.84$; slope, –8.0 mmol K/mol Ca; $P = 0.004$. WT+F: $r = 0.53$; slope, 4.5 mmol K/mol Ca; $P = 0.05$. *Ae2*-null enamel: $r = 0.30$; slope, 7.3 mmol K/mol Ca; $P = 0.51$. *Ae2*-null+F: $r = 0.36$; slope, 7.6 mmol K/mol Ca; $P = 0.28$. (**c**) Correlations between K and Cl in Ae2 group. WT: $r = –0.84$ slope, –0.55 mmol K/mol Cl; $P = 0.004$. WT+F: $r = 0.53$; slope, 0.35 mmol K/mmol Cl; $P = 0.05$. *Ae2*-null enamel: $r = 0.55$; slope, 3.2 mmol K/mmol Cl ; $P = 0.15$. *Ae2a;b*-null+F enamel: $r = 0.81$; slope, 3.0 mmol K/mmol Cl; $P = 0.01$. This figure is available in color online at http://jdr.sagepub.com.

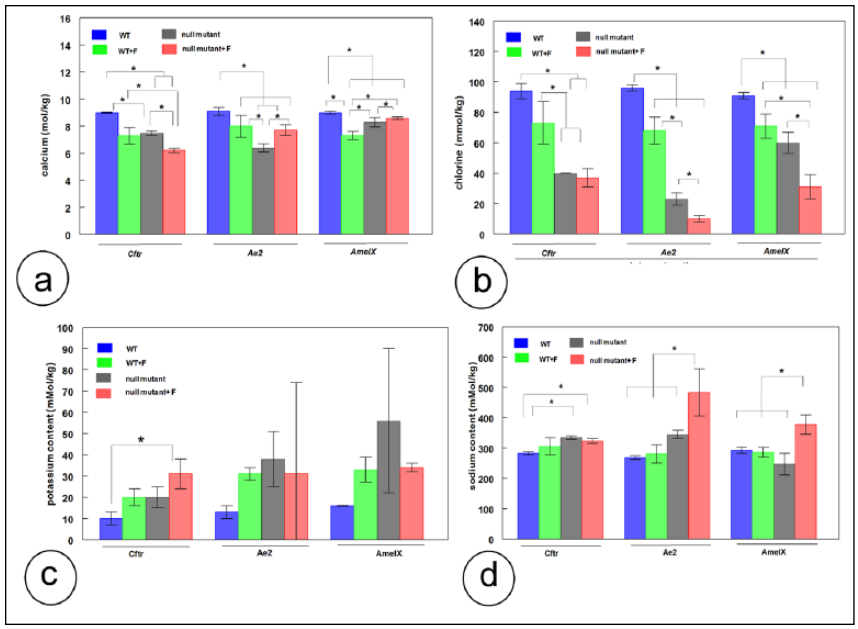

Figure 3. Changes in calcium (**a**), chlorine (**b**), potassium (**c**), and sodium (**d**) in late maturation–stage enamel of lower incisor enamel for the 4 models. Part of the data for calcium and chlorine from panel a have been presented as percentage weight values in table form (Lyaruu et al. 2014; Bronckers et al. 2015) and are shown here for clarity. Blue: wild-type enamel. Green: fluorotic wild-type enamel. Gray: null mutant enamel. Red: fluorotic null mutant enamel. *Cftr*-, *Ae2a,b*-, and *AmelX*-null mutants. Average values and standard deviations (n = 3 to 5 mice), analysis of variance, $^*P < 0.05$ between groups of same genotype. Summary presented in Appendix Table 2. This figure is available in color online at http://jdr.sagepub.com.

Discussion

In this study, we measured the (total) levels of trace elements in forming enamel, as a method to determine which ions were transported through the ameloblast layer into the enamel. Although it has been known that enamel contains low levels of trace elements (Söremark and Grön 1966; Shaw and Yen 1972; Aoba et al. 1992; Lundgren et al. 1998), their significance and interrelationship were unknown. We show that the levels of K^+, Na^+, and Cl^- elements correlate with changes in the levels of Ca^{2+} and HPO_4^{2} and hence likely reflect the activity of mineral ion transporters as Nckx4 and NaPi-2b and pH regulators as Ae2a,b and Cftr.

It is important to note that ion transport is not determined by the total levels (mostly crystal bound as we measured here) but rather by the much lower ionic and unbound levels of Ca^{2+}, Pi, Na^+, K^+, and Cl^- in enamel fluid in contact with the apical plasma membrane of the ameloblasts (Aoba and Moreno 1987). Our analysis is based on the understanding that the trace elements in the soluble pool of enamel fluid are in a dynamic equilibrium with a large pool of bound ions adsorbed to the crystal surface. This bound pool is very motile indicated by the ease by which K^+ and Na^+ can be extracted from finely crushed enamel by water (Aoba et al. 1992). Small changes in pH and ion levels (determined by the dynamics of ion secretion and reabsorption, pH, crystal formation, crystal surface, and adsorption and desorption to crystal surfaces) in enamel fluid near the apical membranes of ameloblasts will influence the activity of the ion transporters.

Ion transporters in transport epithelia respond very rapidly to changes in ion levels in the fluid in contact with the plasma membrane. We did not analyze enamel at the surface but measured enamel halfway between surface and dentin-enamel junction, which reflects changes at the surface at some earlier time. In enamel, trace ions or metal ions can accumulate in forming minerals by which enamel forms a permanent record of compositional changes during development. The changes in K^+ and Na^+ that we found by measuring the composition at the same depth at different times (a *longitudinal* or *function of time* study) are the same as reported for developing porcine enamel for a given age at different depths (a *transversal* study; Aoba et al. 1992). Our measurements in mid enamel hence reflect the same changes in enamel that some time earlier happened at the enamel surface, mediated by the activity of ion transporters in the ameloblast membranes.

The localization of Nckx4 furthermore suggests that ruffle-ended cells are transporting Ca^{2+}, while transport by smooth-ended cells is low or absent. The majority of maturation ameloblasts in rat incisors is ruffle ended (50%) or is becoming ruffle ended (25%), while smooth-ended ameloblasts constitute a minor population (Smith 1998). We found that the majority of maturation ameloblasts were immunopositive for Nckx4 and that the Nckx4-positive ameloblast layer was sometimes interrupted by small groups of Nckx4-negative cells, similar as seen after immunostaining for Ae2 (Bronckers et al. 2009). The immunonegative gaps also resemble the narrow pH neutral bands after staining with pH dyes, areas normally overlain by smooth-ended cells. Collectively, it is plausible that the Nckx4-positive cells are the ruffle-ended cells and the Nckx4-negative cells, the smooth-ended cells. This implies that the ruffle-ended cells are mainly involved in Nckx4-mediated Ca^{2+} transport.

The results also indicate that after secretion of K^+ and Ca^{2+} into forming enamel, the K^+ is continuously removed from the enamel, whereas Ca^{2+} is retained by its incorporation into apatite crystals (Fig. 5). Arguments that support such recycling of K^+ are the much lower levels of K^+ in comparison with Ca^{2+} (cotransport by Nkcx4 expects a 1:1 ratio), the change from a negative correlation between Ca and K in wild-type enamel into a (more) positive one and accumulation of K^+ in enamel during hypomineralization.

NaPi-2b is a Na^+-dependent phosphate transporter regulated by FGF23 and 1,25-dihydroxyvitamin D, known to absorb Pi from the intestinal lumen (Forster et al. 2013; Schiavi et al. 2012). Although NaPi-2b has not been shown to secrete Pi in other tissues, the very high *NaPi-2b* mRNA expression in enamel organs (Lacruz et al. 2012; present study) and the

strong immunostaining for NaPi-2b in apical ameloblast membranes suggest that NaPi-2b may secrete Pi into the enamel space. Secretion of Pi and Na^+ by NaPi-2b could occur if the ionic Pi and Na^+ levels in enamel fluid near the apical plasma membrane are kept very low to create steep downward gradients. This could be achieved if the newly secreted ionic Pi is very rapidly removed from the ionic pool by incorporation into growing apatites, along with a very fast withdrawal of Na^+ from enamel fluid by, for example, apical Nckx4, with its high demand for Na^+ to drive secretion of Ca^{2+} (Fig. 5). The very high slope values and strong positive correlation between Na^+ and Pi found in severely hypomineralized enamel when removal of Na^+ is maximally inhibited indeed suggests that in wild-type enamel, Na^+ is so rapidly removed from the enamel space that Na^+ levels are too low to correlate with Pi.

The molecular mechanism in ameloblasts responsible for removal of K^+ is unclear. Both K^+ and Na^+ accumulate when Cl^- levels are very low, which suggests that Cl^--dependent mechanisms, possibly Na^+, K^+, Cl^- cotransporters (NKCCs) are involved in removing K^+ and/or Na^+ from the enamel space. NKCCs are important regulators in kidney and colon, controlling cell volume and transport of Na^+, Cl^-, and water during growth and development (Payne et al. 1995; Isenring et al. 1998). Removal of water from enamel during maturation stage (Smith 1998) and the fact that formation of subameloblastic cysts after injection of fluoride (Lyaruu et al. 2012) is potentiated by coinjection of furosemide, a well-known inhibitor of NKCCs (Payne et al. 1995; Prostak and Skobe 1996) suggests that NKCCs are also operating in ameloblasts.

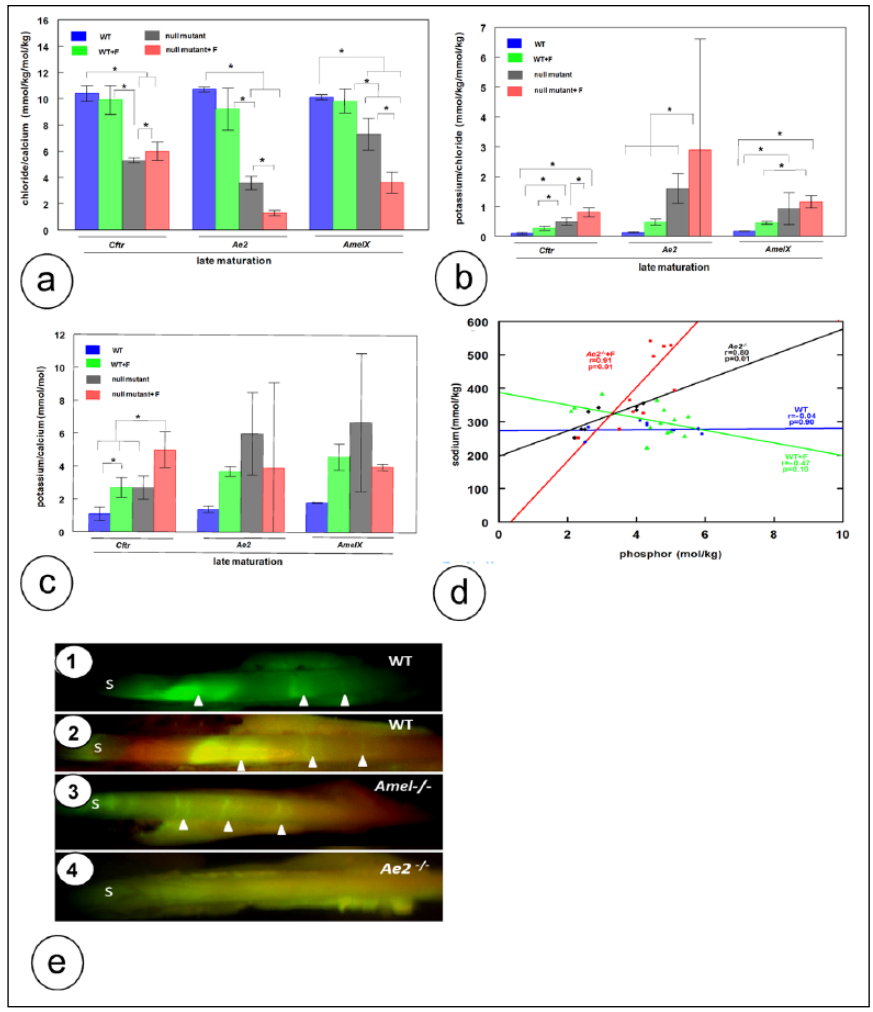

Figure 4. Changes in relative amount of trace elements (**a–c**), correlation between P and Na (**d**), and effect of null mutation of *Amelx* and *Ae2a,b* on modulation (**e**). Effect of *Cftr*-, *Ae2a,b*-, or *Amelx*-null mutation with or without exposure to fluoride on Cl/Ca ratio (a), K/Cl ratio (b), and K/Ca ratio (c) at late maturation (analysis of variance, *$P < 0.05$ between groups of the same genotype). (d) Correlation between Na and P in *Ae2* group. Wild-type (WT) group: $r = 0.04$; slope, 0.71 mmol Na/mol P; $P = 0.90$. WT+F group: $r = 0.47$; slope, −18 mmol Na/mol P, $P = 0.10$. *Ae2a,b*-null group: $r = 0.80$; slope, 38 mmol Na/mol P; $P = 0.01$. *Ae2*-null+F group: $r = 0.91$; slope, 111 mmol Na/mol P; $P = 0.01$. (e) Modulation bands in WT enamel (e1, e2), *AmelX*$^{-/-}$ enamel (e3), and *Ae2*$^{-/-}$ enamel (e4) after injection of calcein. S, secretory enamel. Panel e2 has been stained for 10 s with methyl red and shows the weakly stained (acid, red) wide band of enamel normally overlain by ruffle-ended (RE) ameloblasts. The weakly fluorescent areas (arrowheads) are flanked by 2 fluorescent lines together forming a narrow pH- neutral band that normally is overlain by smooth-ended ameloblasts. This figure is available in color online at http://jdr.sagepub.com.

Ameloblast modulation was affected in all hypomineralization models associated with a drop in Cl^- and a rise in K^+ and Na^+ in the enamel. The rise in K^+ was proportionally much higher than that of Na^+, which makes K^+ a potential candidate involved in regulating ameloblast modulation. Whether elevated levels of K^+ can directly regulate modulation (e.g., by the effect that K^+ can have on membrane potential of the ameloblasts) or whether K^+ accumulates passively as a result of impaired modulation needs further study. In bone-resorbing osteoclasts, acidification of the bone pit releases crystal-bound K^+ (Bushinsky et al. 1997). High K^+ levels depolarize the osteoclast plasma membrane, arrest bone resorption, and induce detachment of the cells from the bone surface (Kajiya et al. 2003). In developing enamel, K^+ adsorbed to crystal surfaces could be released from the crystals into the enamel fluid by gradual acidification during crystal formation, impair recycling of K^+, and reduce or even reverse Ca^{2+} transport, turning the ameloblast from ruffle- to smooth-ended cells (Fig. 5). Excess K^+ could also be washed out along with Na^+, protons, and matrix peptides during modulation when the location of

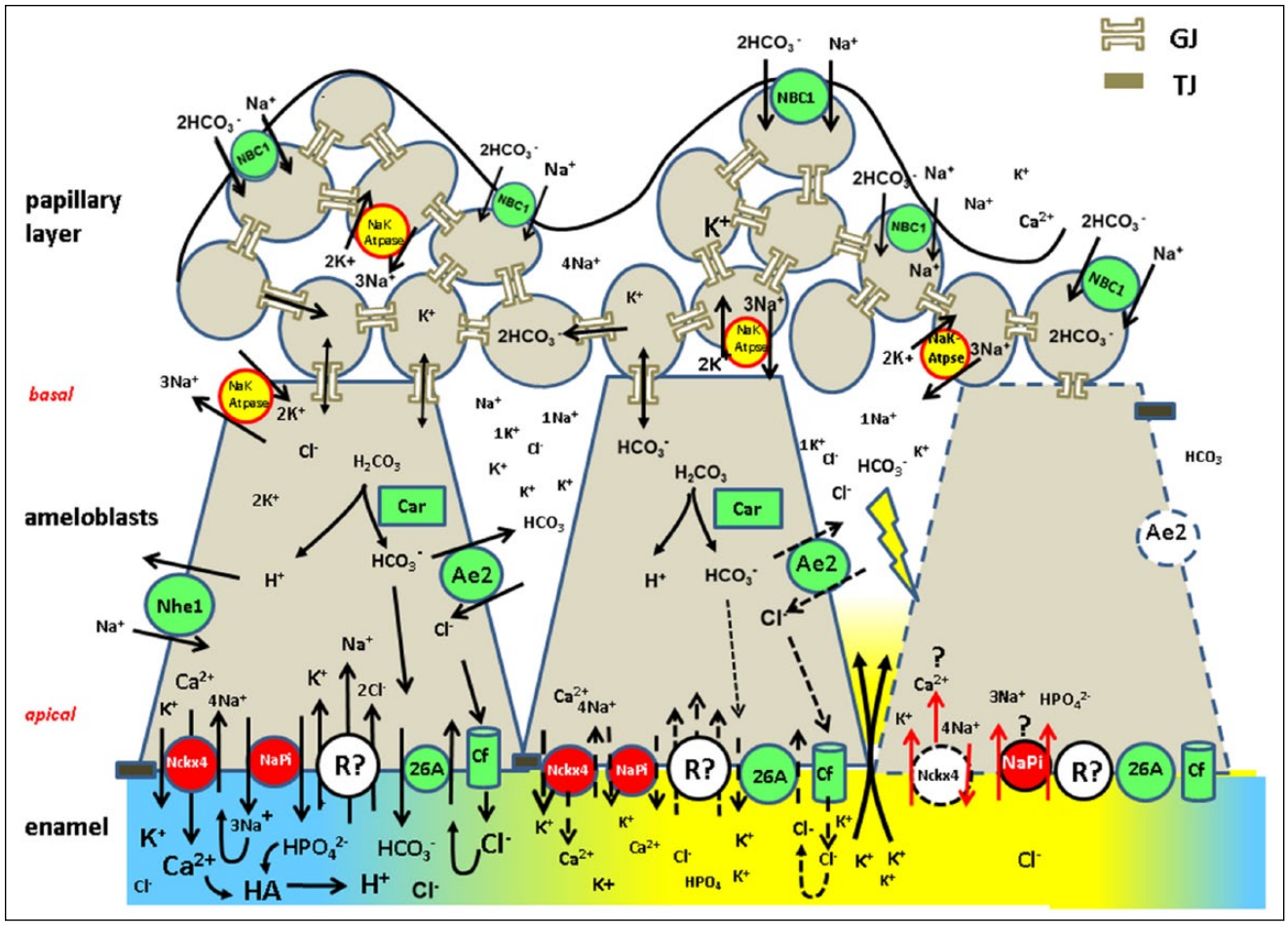

Figure 5. Working model for coordinated transport of Ca^{2+}, Pi, and bicarbonate into enamel in a single modulation cycle. For simplicity, the groups of ruffle- and smooth-ended cells are depicted as 1 cell. Left: ruffle-ended ameloblast at the start of a cycle. Enamel below the ameloblast is pH neutral (blue). A Na^+K^+-dependent Ca^{2+} exchanger (likely Nckx4, in red) transports 1 Ca^{2+} and 1 K^+ in exchange for 4 Na^+. A Na^+-dependent Pi transporter (possibly NaPi-2b, in red) cosecretes 1 Pi with 3 Na^+. For Nckx4 to secrete 1 Ca^{2+} requires uptake of 1 more Na^+ than what NaPi-2b secretes to transport 1 Pi. Intracellular levels of Na^+ and K^+ are tightly regulated by Na^+K^+-ATP-ase in papillary layer and basal portion of the ameloblasts. Formation of hydroxyapatite (HA; left at the bottom) releases protons, which are buffered by secretion of bicarbonates, generated by the pH-regulating machinery (in green). Bicarbonates are generated by carbonic anhydrase 2 (Car) or imported by Nbce1 by ameloblasts and/or by papillary layer cells and transferred through gap junctions (GJ) into ameloblasts. Secretion of bicarbonates into enamel likely involves the Slc26A family (Dra, Slc26a6, pendrin; Jalali et al. 2014, 2015), anion exchanger Ae2, Na^+-hydrogen exchanger 1 (Nhe1), and the cystic fibrosis transmembrane conductance regulator (CF). A major portion of Cl^- is adsorbed to crystals, retained, and in equilibrium with the soluble portion available for exchange for bicarbonate. Na^+, K^+, and Cl^- are recycled by an unknown mechanism (R; possibly members of the NKCC family) to prevent accumulation of K^+ and Na^+ and withdraw fluid. Ameloblast in the middle: Depletion of Cl^- in forming enamel needed to secrete bicarbonate lowers pH in enamel (yellow), delays mineral accretion and reabsorption of K^+ and Na^+, and dissolves immature crystals. Acidification enhances ionic levels of Ca^{2+} and Pi and releases mineral-bound K^+. Increase of Ca^{2+} and Pi in enamel fluid reduce their gradient, slowing down Ca^{2+} transport by Nckx4, and impairs K^+ reabsorption. Ameloblast to the right. K^+ above a threshold level abruptly changes membrane potential (yellow flash) and, with high ionic Ca^{2+}, reverses the Ca^{2+} efflux by Nckx4 into an influx. This sets the cell in crisis and turns it into smooth-ended mode. The cells disassemble their ruffled border, inactivate (green into white) or degrade (broken rim) Ae2 and Nckx4, and displace tight junctions (TJ) from apical into basal position. This briefly opens the enamel space to mix enamel fluid with bicarbonate-rich and K^+-poor intercellular fluid, neutralizing pH and flushing out K^+, Na^+, and matrix peptides (Smith 1998). Some cells will not survive (apoptosis); others will recover, replace the tight junctions back apically, and start a new cycle. This figure is available in color online at http://jdr.sagepub.com.

tight junctions in ameloblasts changes from the apical to the basal border and back again (Smith 1998).

Author Contributions

A.L.J.J. Bronckers, contributed to conception, design, data acquisition, analysis, and interpretation, drafted and critically revised the manuscript; D. Lyaruu, contributed to design, data acquisition, and analysis, drafted and critically revised the manuscript; R. Jalali, B. Zandieh-Doulabi, contributed to design, data acquisition, and analysis, critically revised the manuscript; J.F. Medina, contributed to design and data acquisition, critically revised the manuscript; P.K. DenBesten, contributed to conception, design, data acquisition, analysis, and interpretation, critically revised the manuscript. All authors gave final approval and agree to be accountable for all aspects of the work.

Acknowledgments

We acknowledge W. Lustenhouwer and Dr. S. Matveev (VU University Amsterdam, Amsterdam, Netherlands) for assistance with the microprobe determinations; Drs. S. Sarvide (University of Navarra, Pamplona, Spain), Y. Nakano (University of California, San Francisco, CA, USA), and T. Bervoets (ACTA, Amsterdam, Netherlands) for expert technical help; Drs S. Schiavi and Y. Sabbagh (Genzyme, Sanofi, MA, USA) for providing anti-NaPi-2b; Dr. M. C. Steward (University of Manchester, Manchester, UK) for helpful advice; and Dr. I. Forster (University of Zurich, Zurich, Switzerland) for kindly donating anti-NaPi-2b antibodies. The work was financially supported by the National Institutes of Health (DE13508). The authors declare no potential conflicts of interest with respect to the authorship and/or publication of this article.

References

Aoba T, Moreno EC. 1987. The enamel fluid in the early secretory stage of porcine amelogenesis: chemical composition and saturation with respect to enamel mineral. Calcif Tissue Int. 41(2):86–94.

Aoba T, Shimoda S, Moreno EC. 1992. Labile or surface pools of magnesium, sodium, and potassium in developing porcine enamel mineral. J Dent Res. 71(11):1826–1831.

Arquitt CK, Boyd C, Wright JT. 2002. Cystic fibrosis transmembrane regulator (Cftr) is associated with abnormal enamel formation J Dent Res 81(7):492–496.

Bronckers AL, Lyaruu DM, Guo J, Bijvelds MJ, Bervoets TJ, Zandieh-Doulabi B, Medina JF, Li Z, Zhang Y, DenBesten PK. 2015. Composition of mineralizing incisor enamel in cystic fibrosis transmembrane conductance regulator-deficient mice. Eur J Oral Sci. 123(1):9–16.

Bronckers AL, Lyaruu DM, Jansen ID, Medina JF, Kellokumpu S, Hoeben KA, Gawenis LR, Oude-Elferink RP, Everts V. 2009. Localization and function of the anion exchanger Ae2 in developing teeth and orofacial bone in rodents. J Exp Zool B Mol Dev Evol. 312(4):375–387.

Bushinsky D, Gavrilov K, Chabala JM, Featherstone JD, Levi-Setti R. 1997. Effect of metabolic acidosis on the potassium content of bone. J Bone Min Res. 12(10):1664–1671.

DenBesten P, Li W. 2011. Chronic fluoride toxicity: dental fluorosis. Monogr Oral Sci. 22:81–96.

DenBesten PK, Crenshaw MA, Wilson MH. 1985. Changes in the fluoride-induced modulation of maturation stage ameloblasts of rats. J Dent Res. 64(12):1365–1370.

Forster IC, Hernando N, Biber J, Murer H. 2013. Phosphate transporters of the SLC20 and SLC34 families. Mol Aspects Med. 34(2–3):386–395.

Gawenis LR, Spencer P, Hillman LS, Harline MC, Morris JS, Clarke LL. 2001. Mineral content of calcifying tissues in cystic fibrosis mice. Biol Trace Elem Res. 83(1):69–81.

Guo J, Lyaruu DM, Takano Y, Gibson CW, DenBesten PK, Bronckers AL. 2015. Amelogenins as potential buffers during secretory-stage amelogenesis. J Dent Res. 94(3):412–420.

Hilfiker H, Hattenhauer O, Traebert M, Forster I, Murer H, Biber J. 1998. Characterization of a murine type II sodium-phosphate cotransporter expressed in mammalian small intestine. Proc Natl Acad Sci U S A. 95(24):14564–14569.

Hu P, Lacruz RS, Smith CE, Smith SM, Kurtz I, Paine ML. 2012. Expression of the sodium/calcium/potassium exchanger, NCKX4, in ameloblasts. Cells Tissues Organs. 196(6):501–509.

Isenring P, Jacoby SC, Payne JA, Forbush B. 1998. Comparison of Na-K-Cl cotransporters NKCC1, NKCC2, and the HEK cell Na-K-Cl cotransporter. J Biol Chem. 273(18):11295–11301.

Jalali R, Guo J, Zandieh-Doulabi B, Bervoets TJ, Paine ML, Boron WF, Parker MD, Bijvelds MJ, Medina JF, DenBesten PK, et al. 2014. NBCe1 (SLC4A4) a potential pH regulator in enamel organ cells during enamel development in the mouse. Cell Tissue Res. 358(2):433–442.

Jalali R, Zandieh-Doulabi B, DenBesten PK, Seidler U, Riederer B, Wedenoja S, Micha D, Bronckers AL. 2015. Slc26a3/Dra and Slc26a6 in murine ameloblasts. J Dent Res. 94(12):1732–1739.

Josephsen K, Takano Y, Frische S, Praetorius J, Nielsen S, Aoba T, Fejerskov O. 2010. Ion transporters in secretory and cyclically modulating ameloblasts: a new hypothesis for cellular control of preeruptive enamel maturation. Am J Physiol Cell Physiol. 299(6):C1299–C1307.

Kajiya H, Okamoto F, Fukushima H, Takada K, Okabe K. 2003. Mechanism and role of high potassium induced reduction of intracellular Ca concentration in rat osteoclasts. Am J Physiol Cell Physiol. 285(2):C457–C466.

Lacruz RS, Smith CE, Chen YB, Hubbard MJ, Hacia JG, Paine ML. 2011. Gene expression analysis of early and late maturation stage rat enamel organ. Eur J Oral Sci. 119 Suppl 1:149–157.

Lacruz RS, Smith CE, Kurtz I, Hubbard MJ, Paine ML.2013. New paradigms on the transport functions of maturation-stage ameloblasts. J Dent Res. 92(2):122–129.

Lacruz RS, Smith CE, Moffatt P, Chang EH, Bromage TG, Bringas P Jr, Nanci A, Baniwal SK, Zabner J, Welsh MJ, et al. 2012. Requirements for ion and solute transport, and pH regulation during enamel maturation. J Cell Physiol. 227(4):1776–1785.

Lundgren T, Persson LG, Engström EU, Chabala J, Levi-Setti R, Norén JG. 1998. A secondary ion mass spectroscopic study of the elemental composition pattern in rat incisor dental enamel during different stages of ameloblast differentiation. Arch Oral Biol. 43(11):841–848.

Lyaruu DM, Bronckers AL, Mulder L, Mardones P, Medina JF, Kellokumpu S, Oude Elferink RP, Everts V. 2008. The anion exchanger Ae2a,b$^{-/-}$ mice is required for enamel maturation in mouse teeth. Matrix Biol. 27(2):119–127.

Lyaruu DM, Medina JF, Sarvide S, Bervoets TJ, Everts V, Denbesten P, Smith CE, Bronckers AL. 2014. Barrier formation: potential molecular mechanism of enamel fluorosis. J Dent Res. 93(1):96–102.

Lyaruu DM, Vermeulen L, Stienen N, Bervoets TJ, DenBesten PK, Bronckers AL. 2012. Enamel pits in hamster molars, formed by a single high fluoride dose are associated with perturbation of transitional stage ameloblasts. Caries Res. 46(6):575–580.

Okumura R, Shibukawa Y, Muramatsu T, Hashimoto S, Nakagawa KI, Tazaki M, Shimono M. 2010. Sodium-calcium exchangers in rat ameloblasts. J Pharmacol Sci. 112(2):223–230.

Parry DA, Poulter JA, Logan CV, Brookes SJ, Jafri H, Ferguson CH, Anwari BM, Rashid Y, Zhao H, Johnson CA, et al. 2013. Identification of mutations in SLC24A4, encoding a potassium-dependent sodium/calcium exchanger, as a cause of Amelogenesis Imperfecta. Am J Hum Genet. 92(2):307–312.

Payne JA, Xu JC, Haas M, Lytle CY, Ward D, Forbush B 3rd. 1995. Primary structure, functional expression and chromosomal localization of the bumetanide-sensitive Na-K-Cl cotransporter in human colon. J Biol Chem. 270(30):17977–17985.

Prostak KS, Skobe Z. 1996. Anion translocation through the enamel organ. Adv Dent Res. 10(2):238–244.

Schiavi SC, Tang W, Bracken C, O Brien SP, Song W, Boulanger J, Ryan S, Philips L, Liu S, Arbeeny C, et al. 2012. Npt2b deletion attenuates hyperphosphatemia associated with CKD. J Am Soc Nephrol. 23(10):1691–1700.

Shaw JH, Yen PK. 1972. Sodium, potassium, and magnesium concentrations in the enamel and dentin of human and rhesus monkey teeth. J Dent Res. 51(1):95–101.

Shibasaki Y, Etoh N, Hayasaka Ma, Takahashi M, Kakitani M, Yamashita T, Tomizuka K, Hanaoka K. 2009. Targeted deletion of the tybe IIb Na+-dependent Pi-co-transporter, NaPi-IIb, results in early embryonic lethality. Biochem Biophys Res Commun. 381(4):482–486.

Smith CE. 1998. Cellular and chemical events during enamel maturation. Crit Rev Oral Biol Med. 9(2):128–161.

Smith CE, Nanci A, Denbesten PK. 1993. Effects of chronic fluoride exposure on morphometric parameters defining the stages of amelogenesis and ameloblast modulation in rat incisors. Anat Rec. 237(2):243–258.

Söremark R, Grön P. 1966. Chloride distribution in human dental enamel as determined by electron probe microanalysis. Arch Oral Biol. 11(9):861–866.

Stephan AB, Tobochnik S, Dibattista M, Wall CM, Reisert J, Zhao H. 2011. The Na+/Ca2+ exchanger NCKX4 governs termination and adaptation of the mammalian olfactory response. Nat Neurosci. 15(1):131–137.

Takano Y, Ozawa H. 1980. Ultrastructural and cytochemical observations on the alternating morphologic changes of the ameloblasts at the stage of enamel maturation. Arch Histol Jpn. 43(5):385–399.

Wang S, Choi M, Richardson AS, Reid BM, Seymen F, Yildirim M, Tuna E, Gençay K, Simmer JP, Hu JC. 2014. STIM1 and SLC24A4 are critical for enamel maturation. J Dent Res. 93(7):94S-100S.

Wang SK, Hu Y, Yang J, Smith CE, Nunez SM, Richardson AS, Pal S, Samann AC, Hu JC, Simmer JP. 2015. Critical roles for WDR72 in calcium transport and matrix protein removal during enamel maturation. Mol Genet Genomic Med. 3(4):302–319.

Wright JT, Carrion IA, Morris C. 2015. The molecular basis of hereditary enamel defects in humans. J Dent Res. 94(1):52–61.